UNIVERSITY of York

This is a repository copy of *Factors affecting decolourization efficiency of indigo carmine in a coaxial surface plasma falling film reactor*.

White Rose Research Online URL for this paper:
https://eprints.whiterose.ac.uk/207526/

Version: Published Version

---

**Article:**
Jabbariesgandani, Amirmohammad and Walsh, James L. (2023) Factors affecting decolourization efficiency of indigo carmine in a coaxial surface plasma falling film reactor. Journal of Water Process Engineering. 103632. ISSN 2214-7144

https://doi.org/10.1016/j.jwpe.2023.103632

---

**Reuse**
This article is distributed under the terms of the Creative Commons Attribution (CC BY) licence. This licence allows you to distribute, remix, tweak, and build upon the work, even commercially, as long as you credit the authors for the original work. More information and the full terms of the licence here: https://creativecommons.org/licenses/

**Takedown**
If you consider content in White Rose Research Online to be in breach of UK law, please notify us by emailing eprints@whiterose.ac.uk including the URL of the record and the reason for the withdrawal request.

White Rose university consortium
Universities of Leeds, Sheffield & York

eprints@whiterose.ac.uk
https://eprints.whiterose.ac.uk/

Journal of Water Process Engineering 53 (2023) 103632

Contents lists available at ScienceDirect

Journal of Water Process Engineering

journal homepage: www.elsevier.com/locate/jwpe

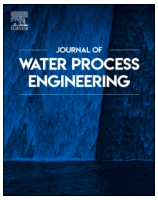

# Factors affecting decolourization efficiency of indigo carmine in a coaxial surface plasma falling film reactor

Amirmohammad Jabbariesgandani [a], James L. Walsh [a,b,*]

[a] Centre for Plasma Microbiology, Department of Electrical Engineering and Electronics, University of Liverpool, Brownlow Hill, Liverpool L69 3GJ, United Kingdom
[b] York Plasma Institute, Department of Physics, University of York, York YO10 5DD, United Kingdom

ARTICLE INFO

*Keywords:*
Indigo carmine
Advanced oxidation processes
Plasma activated water
Falling film reactor

ABSTRACT

Low temperature plasmas generated in close proximity to water offers a convenient means of generating highly oxidising aqueous phase chemical species capable of degrading recalcitrant organic compounds. To ensure the efficacy of the approach the interplay between the plasma excitation parameters and reactor characteristics must be optimised to facilitate efficient generation and transport of reactive chemical species from the plasma phase to the liquid. In this study, indigo carmine dye was used as a model contaminant to investigate factors affecting degradation efficacy in a coaxial falling film reactor coupled to a surface barrier discharge. Plasma generated species in the gas phase were characterised using Fourier transform infra-red spectroscopy and linked to aqueous phase species in the exposed solution. Parameters including dissipated power, pulse width modulation and reactor sealing conditions were systematically investigated to reveal a maximum decolourisation efficiency of 20.18 g/kWh. Through a comparison with other plasma-based and non-plasma-based advanced oxidation processes it was revealed that the coaxial surface barrier falling film reactor developed in this study is highly competitive and worthy of further investigation.

## 1. Introduction

Organic dyes used in a vast number of industrial processes create major issues if released into the environment [1]. Among these dyes, indigo carmine, also known as acid blue 74, is widely used in the textile industries and it is estimated that about 10–15 % of the generated effluent is released into natural water sources [2]. Despite the recalcitrant organic pigment being known to cause serious issues to the respiratory system of humans, and in the case of physical contact, can cause eye and skin irritation; it remains widely used [3]. Thus, elimination of indigo carmine and similar compounds is of high significance.

Traditional methods of wastewater treatment are not typically efficient at decomposing resistant compounds such as organic dyes due to the inherent stability of their chemical structure [4]. In general, organic dyes are not biodegradable and the use of physicochemical processes, such as coagulation, membrane filtration, and flotation can be costly to operate or have the disadvantage of producing secondary waste products, potentially requiring further treatment [5,6]. It is therefore clear that there remains a need to develop more effective, simple, and economical process.

In recent years, emerging methods collectively known as Advanced Oxidation Processes (AOPs) have been employed for the elimination of recalcitrant chemical compounds due to their high capability of removing organic contamination in water [7]. AOPs are mainly based on the in-situ generation of OH radicals which have an extremely high oxidation potential ($E^0 = 2.8$ V/SHE) [8]. In these processes, complete degradation of the molecule is achievable with the further benefit of no sludge being formed as complete mineralization yields only $CO_2$, $H_2O$ and other inorganic compounds [9]. AOPs have been widely investigated for the decomposition of organic dyes, including indigo carmine [10]. Of all the potential AOP technologies currently under investigation, Non-Thermal Plasma (NTP) has been shown to be extremely versatile, capable of degrading a plethora of organic contamination in wastewater using only air and electricity, meaning it can be created on demand and directly at the point of need [11–13].

NTP is a state of matter that is far from thermodynamic equilibrium.

*Abbreviation:* RONS, Reactive Oxygen and Nitrogen Species; SBD, Surface Barrier Discharge; AOP(s), Advanced Oxidation Process(es); NTP, Non-Thermal Plasma; FTIR, Fourier-transform infrared spectroscopy; PWM, Pulse width modulation; OES, Optical emission spectroscopy; DBD, Dielectric barrier discharge; SPS, Second Positive System.

* Corresponding author.
*E-mail addresses:* jlwalsh@liverpool.ac.uk, james.l.walsh@york.ac.uk (J.L. Walsh).

https://doi.org/10.1016/j.jwpe.2023.103632
Received 18 July 2022; Received in revised form 3 March 2023; Accepted 3 March 2023
Available online 20 March 2023
2214-7144/© 2023 The Author(s). Published by Elsevier Ltd. This is an open access article under the CC BY license (http://creativecommons.org/licenses/by/4.0/).

The temperature of heavy species, such as neutrals and ions, are close to ambient [14]; while electrons typically have temperatures in the 1–5 eV range (1 eV = 11,606 K). Energetic electrons take part in ionisation reactions that sustain the plasma and are also able to dissociate and excite molecules in the background gas, creating a complex mixture that is rich in highly-reactive chemical species. In NTP created in humid air, reactive chemical species such as $OH^{\bullet}$, $H_2O_2$, O, $O_3$, $NO^{\bullet}$, $NO_2$ and $NO_3$ are produced, and are collectively termed Reactive Oxygen and Nitrogen Species (RONS). In addition to RONS, such plasmas also produce UV radiation and intense electric fields, that can be utilized to enhance the removal of microbial and viral contamination [15–20]. In the context of wastewater treatment, NTP's have shown considerable promise for the removal of refractory compounds as hydroxyl radicals are produced more efficiently compared to conventional AOPs [21–23]. Some of the important general reactions that occur in atmospheric air plasma are listed below (Eq.1 to Eq.13).

$$e^{-*} + O_2 \rightarrow O^{\cdot} + O^{\cdot} + e^{-} \quad (1)$$

$$O^{\cdot} + O_2 + M \rightarrow O_3 + M \quad (2)$$

$$e^{-*} + H_2O \rightarrow OH^{\cdot} + H^{\cdot} + e^{-} \quad (3)$$

$$2OH \rightarrow H_2O_2 \quad (4)$$

$$e^{-*} + 2H_2O \rightarrow H_2O_2 + H_2 + e^{-} \quad (5)$$

$$e^{-*} + N_2 \rightarrow 2N^{\cdot} + e^{-} \quad (6)$$

$$N^{\cdot} + O \rightarrow NO \quad (7)$$

$$O^{\cdot} + NO \rightarrow NO_2 \quad (8)$$

$$O_3 + NO \rightarrow NO_2 + O_2 \quad (9)$$

$$NO_2 + N \rightarrow N_2O + O \quad (10)$$

$$NO_3^{\cdot} + NO_2 + M \rightarrow N_2O_5 + M \quad (11)$$

$$NO_2 + O + M \rightarrow NO_3^{\cdot} + M \quad (12)$$

$$OH^{\cdot} + NO_2 \rightarrow HNO_3 \quad (13)$$

A potential disadvantage of NTP-based AOPs is that the efficiency of the process is strongly influenced by several factors including reactor configuration, electrical characteristics of the plasma generating source, and the chemical characteristics of the contamination [24]. Malik highlighted these issues in a study that considered 27 distinct NTP reactors reported in the literature, the review highlighted that the efficiency of the examined systems at removing organic contamination from water varied by an enormous six orders of magnitude [11]. Reactors which involved the spraying of contaminated water though an NTP were found to be the most efficient, while reactors which created a plasma close to, but not in direct contact with, contaminated water were found to be the least efficient [25].

Based on the efforts of Malik and others, a considerable amount of research over the past decade has been directed toward the further development of direct-contact NTP reactors. Despite these efforts and the exceptional efficiencies reported in laboratory-based tests, the direct contact between NTP and liquid introduces a number of challenges. The characteristics of the NTP, and therefore its chemical composition, are directly linked to the electrical properties of the contaminated water, which inevitably varies. Furthermore, the use of short-duration high voltage pulses to generate NTP is considered the most effective approach, yet the generation of such pulses to create uniform NTP in a large volume is particularly challenging.

Given the drawbacks and challenges associated with direct-contact NTP reactors, several recent studies have re-visited the use of in-direct NTP systems for water treatment [26]. In particular, the Surface Barrier Discharge (SBD) configuration enables large volume NTP generation in humid air with modest power supply requirements. One drawback of the indirect approach is that the mass-transport of highly reactive RONS, such as O and $OH^{\bullet}$, is limited by the air-gap between the plasma and liquid phases. Despite this challenge, studies have shown the SBD configuration can be effective; for example, Yonezawa and colleagues used an SBD flowing film reactor to remove indigo carmine (20 mg/L) using sinusoidal excitation and obtained a decolourisation rate of 99.3 % using 2.91 Wh of electricity. To maximise the efficiency of an in-direct NTP reactor the mass transport of RONS from the NTP to the liquid must be optimised. One particularly convenient method to achieve this is through the use of a falling film reactor [27], whereby a thin liquid film flows in close proximity to an NTP source. Such reactors have been used extensively in direct-contact NTP studies [28,29], but have not yet been used for the in-direct NTP treatment of contaminated water.

This contribution considers the hypothesis that the efficiency of in-direct NTP wastewater treatment processes can rival that of direct-contact treatment processes by combining a falling film reactor with an SBD. To test the hypothesis, the decolourisation of indigo carmine dye was examined as a function of plasma operating parameters whilst the generation of RONS was assessed in both the liquid and gas phases.

## 2. Materials and methods

### 2.1. NTP reactor and plasma source

The NTP reactor used in this study consisted of two coaxial quartz tubes, an SBD electrode, a high voltage power supply, a liquid circulation pump with a 0.3 L/min flow rate and a liquid storage tank (Fig. 1). The inner and outer quartz tubes had a diameter of 14 mm and 30 mm, respectively. In order to align the tubes coaxially, two perforated holders were placed above and below the plasma generating electrode. The SBD device was constructed around the outer quartz tube and featured two electrodes, an outer electrode that comprised of a copper sheet connected to the high-voltage power supply, and a grounded hexagonal stainless-steel mesh on the inside of the tube. On application of a sufficiently high voltage time-varying signal from the power source, NTP was observed to form within the hexagonal mesh, Fig. 1b. With the pump energised, the sample solution was pushed up through the inner tube at a constant flow of 5.30 mL/s; at the top of the tube, the liquid flowed over the edge to form a uniform thin film on the outer side of the tube, in close proximity to the NTP generating electrode.

Experiments were performed in both sealed and unsealed reactor configurations as it is known that RONS generation in air plasma is highly sensitive to the composition of the background air. In the sealed mode, the top part of the reactor was sealed with an air tight plug to trap plasma generated species within the reactor. In contrast, the reactor was left open to the ambient laboratory air in the unsealed mode.

The NTP power source comprised of a custom-made high voltage generator delivering a sinusoidal waveform with a variable amplitude from 1 to 20 kV at a constant frequency of 12 kHz. An oscilloscope (Keysight EDUX1002A) was used with a high voltage probe (Testec model TT-HVP 15HF) and Pearson current monitor (Pearson model 2877) to measure the voltage applied to the electrode and the resulting current, respectively. Figure SI1 in the supplementary material shows current and voltage waveforms for the eight cases considered in this study. Power dissipated within the plasma was calculated by multiplying the current and voltage waveforms to reveal the instantaneous power, which was subsequently averaged over multiple cycles of the applied voltage to determine the time-averaged dissipated power.

### 2.2. Pollutant

Indigo carmine dye, 5.50-indigodisulfonic acid sodium salt ($C_{16}H_8N_2Na_2O_8S$, ACROS Organics™) solution was used as the model

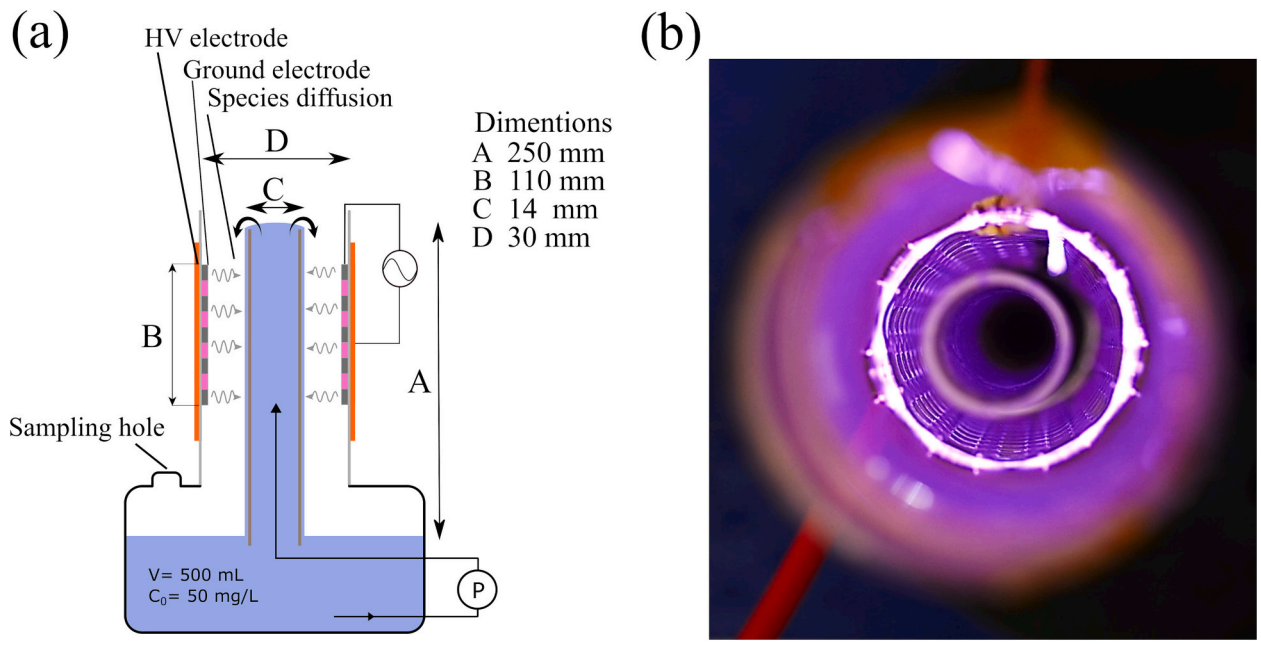


**Fig. 1.** Atmospheric pressure air plasma created using a surface barrier discharge coupled to a coaxial falling film: (a) Schematic showing reactor configuration and key dimensions, and (b) photo of plasma generated in the reactor at 20 W.

pollutant for all experiments. An aqueous solution was made by dissolving 50 mg of the dye in one litre of deionized water created using a reverse osmosis filter (SUEZ Water Technologies & Solutions). For all experiments, the total volume of the circulating solution was 500 mL.

### 2.3. Decolourisation ratio and efficiency

The decolourisation ratio was defined as the concentration of dye remaining after NPT treatment, divided by the intial concentration and expressed as a percentage; while the decolourisation efficiency was defined as the decolourised amount (grams) of dye divided by the input power, using the following equations (Eq. 14 & 15), respectively.

$$\text{Decolourisation ratio } (\%) = \frac{C_0 - C_t}{C_t} \times 100 \quad (14)$$

$$\text{Decolourisation efficiency } (g/kWh) = \frac{0.5 \times C_0 \times V_0}{P \times t_{50}} \quad (15)$$

where $C_0$ is the initial concentration of the dye (50 mg/L), $C_t$ is the concentration of the dye at time t, $V_0$ is the total volume of the dye solution in the reactor (500 mL), P is the input energy in kW, and $t_{50}$ is the time in hours when 50 % of the dye is decoloured. $C_t$ was obtained by measuring the absorbance value of indigo carmine at 610 nm by UV–Vis spectrometer and then using the calibration curve of indigo carmine, Figure SI2, [30]. The $G_{50}$ values for this work used in the comparative study section (Section 3.4) were calculated using the time-averaged dissipated power. In comparative studies where the $G_{50}$ value was not given, the reported time averaged power was used, or was calculated for pulsed discharges using the quoted energy per pulse multiplied by the pulse repetition frequency.

### 2.4. Gas phase species detection and quantification

The detection of the long-lived plasma species in the gas phase was performed by Fourier Transform Infra-Red (FTIR) spectroscopy. The effluent gas containing plasma species in the reactor was pumped to a short-path gas cell (10 cm) comprised of KBr windows by a small gas pump. The IR absorption spectra was recorded by a Jasco FT/IR-4000 spectrometer at three-minute intervals. The spectral window was set in the range of 500 $cm^{-1}$ to 4000 $cm^{-1}$, the number of acquisitions was set to 16 and the duration of the acquisition for each spectrum was 3 s.

Ozone measurements were carried out in both the sealed and unsealed reactor configuration. In the unsealed configuration, ozone was measured using an ozone monitor (2B technologies, model 106-M) with a minimum flow rate of 0.3 L/min. In the sealed configuration, ozone was measured in real time using UV absorption at 254 nm. To conduct the measurement a 600 $\mu m^2$ optical fibre was connected to a UV lamp (Ocean Optics Deuterium lamp DH-2000-CAL) with its open end mounted in the cap of the NTP reactor, a second 600 $\mu m^2$ optical fibre was connected to an Ocean Optics spectrometer (USB2000+) with its open end mounted in the cap of the reactor. The free-space, i.e. absorption, path length between the two fibres was 5 mm. Using the Beer-Lambert law with the absorption cross-section of $1.1329 \times 10^{-17}$ $cm^2 \cdot molecule^{-1}$ the absolute concentration of ozone was calculated. The Ocean Optics spectrometer was also used to capture light emission from the plasma to assist in identification of excited species.

### 2.5. pH and conductivity measurement

The pH and electrical conductivity (σ) of NTP treated liquids were measured using a combined pH and conductivity meter (Hanna Instruments 9813-6 with pH probe HI-1285-6). The instrument was calibrated using standard buffer solutions (pH = 4.01 and 7.01) for pH, and standard conductivity solution (1413 μS/cm) before taking measurements. The pH and conductivity values were recorded at five-minute intervals for all tests conducted.

### 2.6. Nitrites ($NO_2^-$) and Nitrates ($NO_3^-$) quantification

The Griess reagent (Sigma, G4410 at 40 mg/mL) was utilized to quantify $NO_2^-$ concentration in samples through the diazotization reaction. The reagent is composed of two parts in acidic condition which are sulphanilic acid and N-(1-naphthyl) ethylenediamine dihydrochloride. In the colourimetric assay, diazonium salt, which is the product of the sulphanilic acid and nitrites reaction, reacts with N-(1-naphthyl) ethylenediamine dihydrochloride to form an azo dye developing a pink colour in the absorbance range of 548 nm. The corresponding $NO_2^-$ concentration was then obtained using $NaNO_2$ and a Griess reagent

solution (Vol 1:1) calibration curve.

Nitrate ($NO_3^-$) quantification was carried out by spectrophotometric analysis using sodium salicylate (0.5 g/100 mL, Sigma Aldrich, CAS 54-21-7) under very acidic conditions ($H_2SO_4$, Sigma Aldrich) [31]. A standard solution of $KNO_3$ was prepared to create a calibration curve in order to obtain the corresponding $NO_3^-$ concentrations using absorption 415 nm.

## 3. Results

### 3.1. Evolution of gas phase reactive species

The decolourisation of indigo carmine follows the homolytic cleavage of the carbon double bond at the centre of its chemical structure which can be initiated by active species attack [32]. In order to understand the factors affecting the degradation efficacy of indigo carmine, or any other organic pollutant, it is first vital to understand the evolution of key RONS as they are generated and transported from the plasma phase to the aqueous medium.

Within the plasma region a large number of excited and ionized states are produced via direct electron impact. Indeed, OES was used to examine light emission from the plasma operating under different power conditions and revealed dominant emission from the $N_2$ Second Positive System [SPS], Figure SI3. Interestingly, no atomic oxygen emission was observed at 777 nm. This finding indicates that although ground state atomic oxygen must be created in the discharge, evidenced by the copious amount of ozone produced, it is not in an excited state. Beyond the visible plasma region, many species produced in the discharge react to form intermediaries, such as ozone and nitric oxide, which are able to diffuse toward the liquid surface.

Ozone is a long-lived and highly oxidative molecule that can be produced in abundance by NTP generated in atmospheric pressure air. Fig. 2 shows the evolution of ozone density in the reactor in both the sealed and unsealed configuration. Under low discharge power conditions, 5 W, the ozone concentration was observed to increase up to a maximum of approximately 760 ppm in both the sealed and unsealed configuration after approximately 23 min of plasma generation, followed by a plateau, Fig. 2a. In contrast, the evolution of $O_3$ in the 10 W and 20 W cases shows a marked difference, whereby the density reaches a peak then rapidly decreases. For instance, at a dissipated power of 20 W in the unsealed reactor the $O_3$ density reached 570 ppm within 2 mins and was followed by a sharp decrease, dropping to approximately 100 ppm within 8 mins.

To explain the evolution of ozone under the different test conditions, its formation and loss pathways must be considered. In atmospheric pressure air plasma the major production pathway of $O_3$ follows a two-step process; initially, $O_2$ is dissociated by energetic electrons in the plasma leading to the formation of highly reactive atomic oxygen which subsequently reacts with $O_2$ to form $O_3$ [20]. The major loss pathway of $O_3$ involves its reaction with NO, leading to the formation of $NO_2$ and $O_2$. Regardless of the dissipated plasma power, Fig. 2 indicates that $O_3$ is readily produced when plasma is first ignited; however, under higher power operation the density of $O_3$ is seen to reach a maxima and then reduce, in a process known as ozone quenching [33]. As the power dissipated in the plasma is increased the population of vibrationally excited nitrogen ($N_2(\nu)$) grows, this acts to increase the production of NO through the reaction $N_2(\nu) + O \rightarrow NO + N$ ($k = 1 \times 10^{-17}\ m^3 \cdot s^{-1}$) [34]. Park et al. found that the production rate of NO is directly related to the vibrational temperature of $N_2$ molecules, $T_\nu$ [35]. In this investigation, an increase in discharge power likely caused an increase in $T_\nu$, leading to the generation of more NO and subsequent quenching of $O_3$. Notably, this phenomenon can also explain the differences observed in $O_3$ evolution between the sealed and unsealed reactor configurations. In the sealed configuration, NO and $O_3$ were confined to the relatively small volume between the SBD electrode and liquid film, where the elevated temperature could enhance their reaction. Conversely, in the

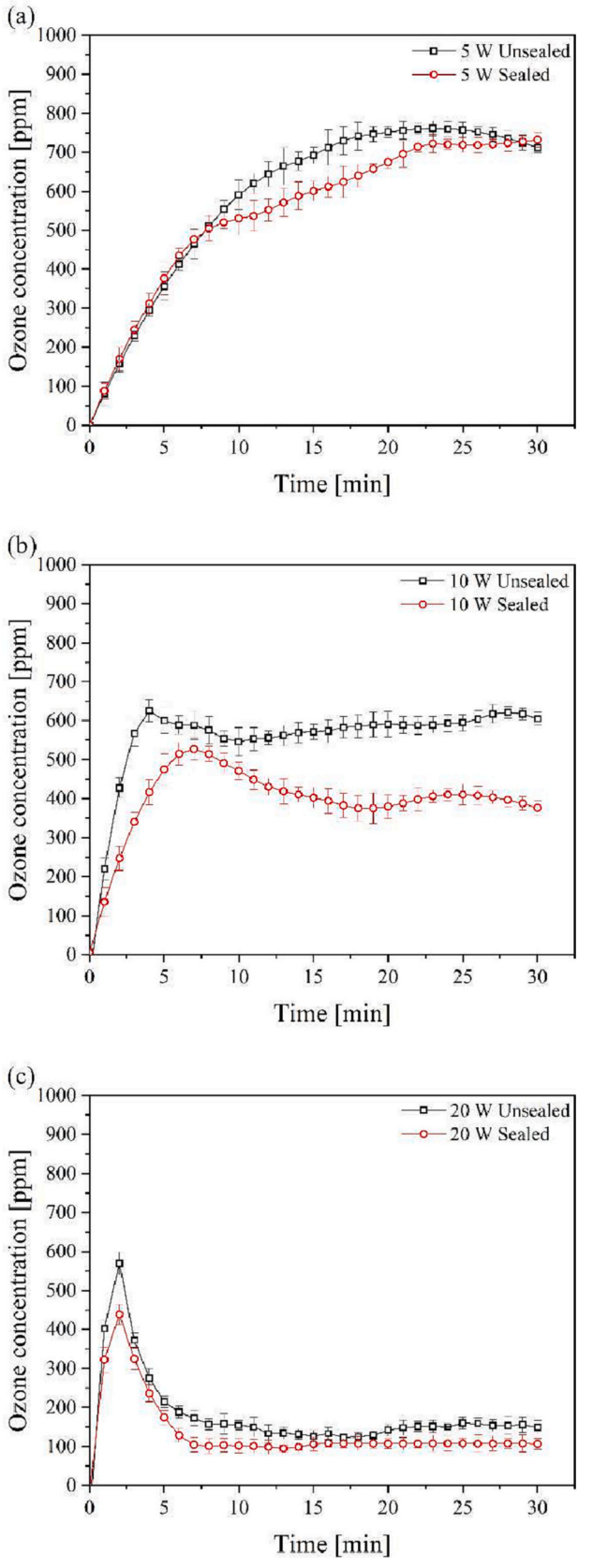


**Fig. 2.** Influence of plasma power on temporal evolution of ozone density at operating powers of: (a) 5 W, (b) 10 W, and (c) 20 W.

unsealed configuration, $O_3$ and NO were able to diffuse beyond the confines of the reactor into the ambient temperature environment, acting to reduce the quenching effect.

FTIR analysis was performed to further examine the composition of gas phase species in the reactor, Fig. 3. The results reveal characteristic absorption peaks for Ozone (~1050 $cm^{-1}$ and ~ 2100 $cm^{-1}$) and $N_2O$ (~1270 $cm^{-1}$ and 2200 $cm^{-1}$), as well as water (1640 $cm^{-1}$) [36]. It can be seen that absorption by ozone decreased with increasing plasma power, signifying a reduction in $O_3$ density. While, the $N_2O$ absorption peak increased slightly with increasing discharge power signifying a modest increase in density.

Notable by its absence from Fig. 3b and Fig. 3c is $NO_2$, a finding that is at odds with the previously described $O_3$ quenching mechanism and other reports in the literature detailing the FTIR spectra of NTP generated in ambient air [37]. Critically, the absence of $NO_2$ in the effluent of the reactor can be explained by considering the presence of the flowing liquid film, which is not a common feature in previously reported studies employing FTIR. It is well known that $NO_2$ readily reacts with water to form a number of aqueous phase species. In the falling film reactor considered in this investigation it is assumed that the $NO_2$ produced by the discharge rapidly reacted with the liquid film, whereas $N_2O$ does not react with water and is less soluble [38], hence $N_2O$ was detected in the reactor effluent and not $NO_2$. This hypothesis was confirmed by running the reactor in the absence of liquid, with the results indicating a strong $NO_2$ peak being observed under high power conditions, Fig. SI4.

### 3.2. *Impact of discharge power and reactor configuration on decolourisation rate*

Fig. 4 highlights the impact of discharge power, pulse modulation and reactor sealing condition on the energy consumption of indigo carmine decolourisation. Regardless of the conditions used, complete decolourisation of indigo carmine was observed; however, in all cases more energy was required to obtain total decolourisation when using a higher discharge power. Fig. 4a shows the decolourisation as a function of energy consumption using continuous electrical excitation with the reactor unsealed, from the figure it is clear that lower dissipated powers improved the electrical efficiency of decolourisation, with the 5 W case showing the highest efficiency of all cases examined. As the 5 W case was found to produce the highest concentration of $O_3$ over the duration of the test, Fig. 2, it is assumed that $O_3$ plays a major role in the decolourisation process, a finding in line with previous works exploring plasma mediated dye colourisation [39].

Fig. 4b shows the impact of sealing the reactor on decolourisation rate. Interestingly, at a dissipated power of 5 W the sealed reactor showed the highest decolourisation rate, while in the unsealed reactor the higher power conditions exhibited the highest decolourisation rate. These observations can be explained by considering the gas phase chemistry described in Fig. 2 and 3. Under low power conditions, $O_3$ quenching does not occur in either the sealed or unsealed configuration, therefore sealing the reactor is beneficial as it prevents the loss of oxidative species from the reactor to the environment. In contrast, under high power conditions sealing the reactor was found to have a detrimental impact on $O_3$ production, Fig. 2, which directly reduces decolourisation efficacy.

Fig. 4c shows the influence of pulse width modulation (PWM) on decolourisation in the unsealed reactor configuration. The results indicate that PWM had a slight positive impact on the electrical efficiency of the decolourisation for both the 5 and 10 W cases. Similar results have been reported in previous studies albeit using different pollutants and reactor configurations. For example, Olszewski et al. investigated the decolouration of methylene orange using a pulse modulated SBD positioned above a stirred liquid volume [32]. They observed that decolouration process was more efficient in PWM mode compared to the continuous mode, attributing this to the low temperature operation associated with PWM acting to reduce both thermal degradation of $O_3$

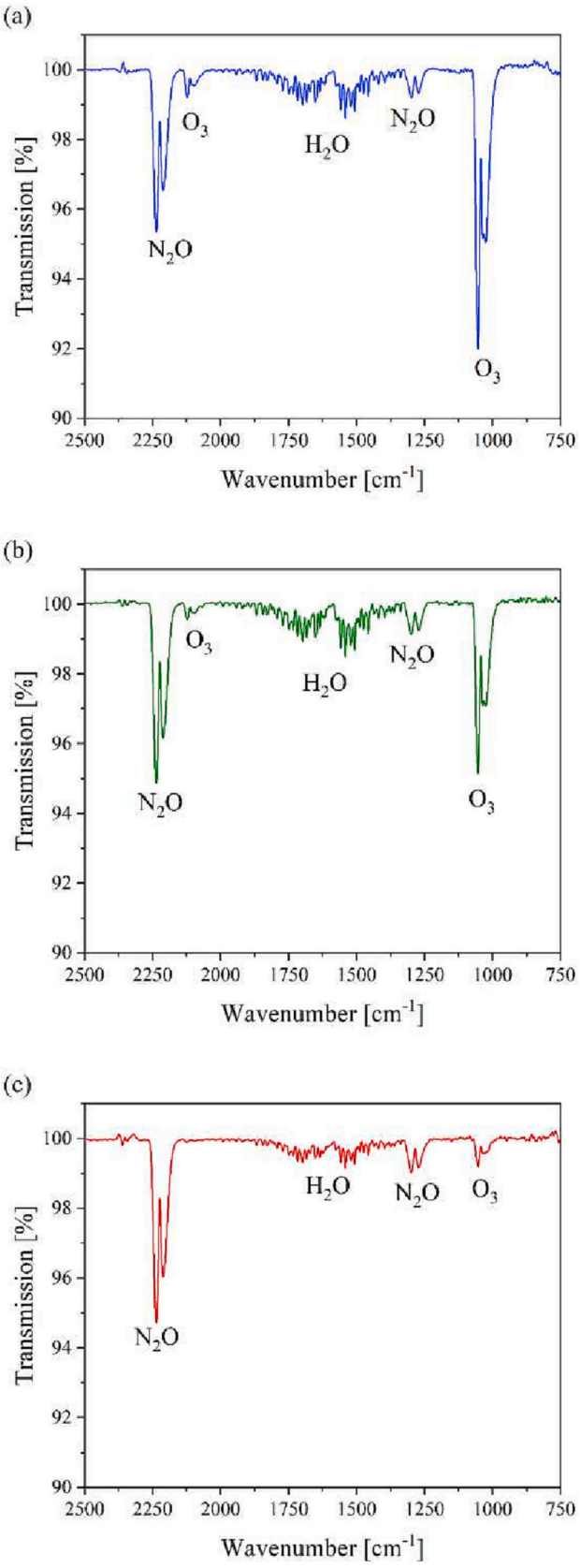


**Fig. 3.** FT-IR transmission spectra showing gas phase species drawn from the reactor after 12 min of plasma generation at discharge powers of: (a) 5 W, (b) 10 W, and (c) 20 W.

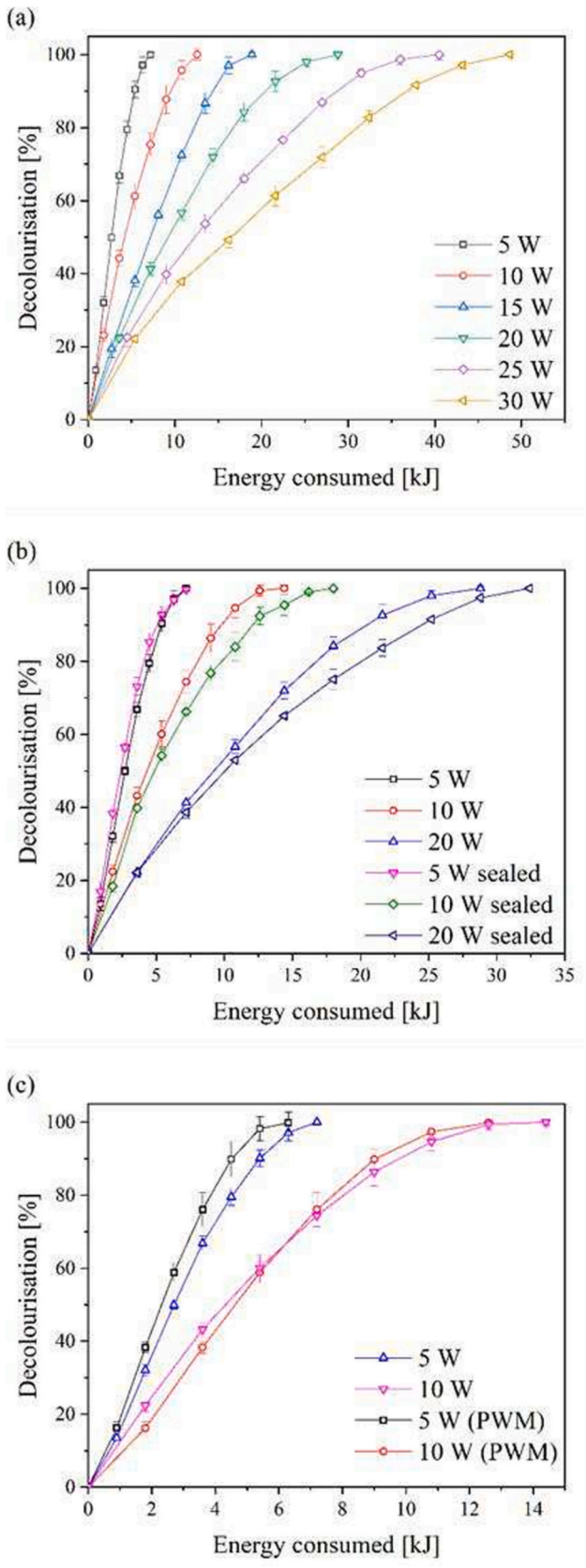


**Fig. 4.** Influence of energy consumption on decolourisation rate, showing the impact of: (a) dissipated plasma power, (b) reactor sealing conditions, and (c) pulse width modulation.

and its quenching.

### 3.3. Aqueous phase chemical assays

It is well known that short-lived and charged species generated by an SBD, such as OH and $HO_2$, do not propagate a significant distance beyond the visible plasma region; consequently, only longer-lived species, including $N_2O$, NO, $NO_2$ and $O_3$, reach the liquid interface where they can diffuse to the liquid bulk and change its properties [39]. To investigate the impact of plasma exposure on the composition of the exposed liquid, the pH, conductivity, nitrite concentration and nitrate concentration were measured in the unsealed operating mode, Fig. 5. The initial pH for all experiments was found to be 6.8. It is commonly known that when water is exposed to air plasma, the pH drops [22].The discharge power had a significant impact on the final pH of the treated solution, Fig. 5a, with the lowest pH of 2.7 being reached after 30 mins of exposure at 20 W dissipated power, while a pH of 3.4 was reached after 30 min at 5 W dissipated power. In line with the drop in pH, the conductivity of the treated solution was observed to increase in all cases, Fig. 5b. The maximum conductivity reached after a 30 min exposure at 20 W was 0.73 mS/cm at 30 min using 20 W.

As shown in Fig. 5c, the concentration of nitrites initially increased for all cases. However, the nitrite concentration remained almost constant or even reduced after 20 mins for the 10 W and 20 W cases. This unexpected trend can likely be attributed to the oxidoreduction of nitrite with $O_3$ to produce nitrate, $NO_2^- + O_3 \rightarrow NO_3^- + O_2$. Critically, this trend was less obvious in the sealed mode of operation, where less ozone is produced at higher operating powers, Fig SI5.

### 3.4. Comparative study

To understand how the efficacy of the SBD falling film reactor compares against other plasma-based and non-plasma-based AOPs a comparison of indigo carmine decolourisation efficiency was compiled using studies found in the literature [10,32,40–48]. Fig. 6 shows the $G_{50}$ (g/kWh) values, i.e. the energy consumed to decompose one gram of pollutant, versus the time needed to reach 50 % decomposition ($t_{50}$). The highest efficiency value ($G_{50}$) in this work was 20.18 g/kWh, achieved using an unsealed reactor operated with a pulse modulated waveform, which achieved a $t_{50}$ in 7.43 mins. The figure clearly indicates that the approach adopted in this work compares favourably to many other non-plasma based AOPs such as UV, UV/ $H_2O_2$ [42], $H_2O_2$/photo Fenton, UV/$TiO_2$ and Fenton/photo Fenton [10]. For example, Rodriguez et al. investigated the decolourisation of indigo carmine in an acidic medium (pH = 5) by irradiating it with UV light using a polychromatic UV high-pressure mercury lamp with and without the presence of hydrogen peroxide. It was demonstrated that decolourisation of IC ($9 \times 10^{-5}$ mol. $L^{-1}$) in the presence of $H_2O_2$ ($16 \times 10^4$ mol.$L^{-1}$) was more efficient than without hydrogen peroxide and the same UV irradiation power. The calculated $G_{50}$ efficiency values were 9.18 g/kWh and 2.28 g/kWh for UV/ $H_2O_2$ and UV, respectively. Palma-Goyes et al. compared three different AOPs: $H_2O_2$/photo Fenton, UV/$TiO_2$ and Fenton/photo Fenton. Among these methods, Fenton/Photo Fenton ($Fe^{2+}$ = 5 mg/L) was the most efficient method to decolourise indigo carmine with a $G_{50}$ value of 1.88 g/kWh, compared to 0.054 g/kWh and 0.06 g/kWh for $H_2O_2$/ photo Fenton ($H_2O_2 = 2.03 \times 10^{-3}$ M) and UV/$TiO_2$ ($TiO_2$ = 1 g/L), respectively.

For plasma based AOPs, Mededovic and Takashima investigated the decolourisation of indigo carmine (20 mg/L) by direct pulsed discharge using various storage capacitors in a point to plate electrode configuration. They reported that indigo carmine decolourisation with a $t_{50}$ of 9 mins and a calculated $G_{50}$ of ~0.0504 g/kWh [46]. Crema et al. also investigated the decomposition of indigo carmine in a cylindrical point to plate gas discharge over the solution using a pulsed discharge in the presence of $O_2$ and $N_2$. It was concluded that using bubbled $O_2$ was the most efficient approach, yielding a $G_{50}$ value of 4 g/kWh [41]. Morimoto

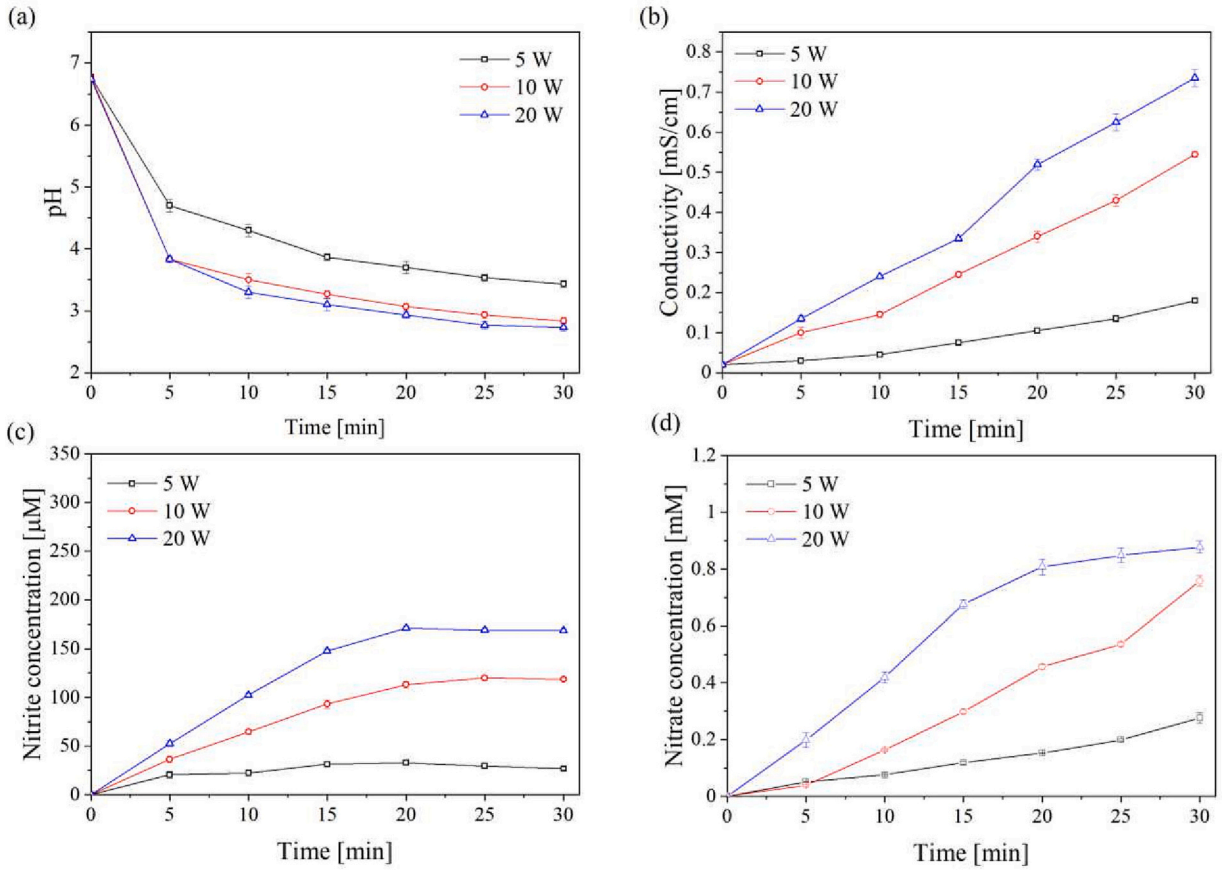


**Fig. 5.** Kinetic evolution of liquid composition under varying plasma generation conditions in the unsealed mode, showing impact on: (a) pH, (b) conductivity, (c) nitrite concentration, and (d) nitrate concentration.

et al. employed a nanosecond pulsed plasma discharge using a stainless steel wire to cylinder falling film DBD reactor. In their study, oxygen gas was used and showed excellent decolourisation efficiency ($G_{50}$ = 24.84 g/kWh) [48].

From the comparative study it is clear that plasma-based methods are extremely promising for the degradation of recalcitrant components, such as organic dyes, in comparison to many other AOP's that are currently under investigation. Among plasma-based processes, the use of an SBD coupled to a falling film reactor was found to offer comparable performance to several other approaches that employ a configuration facilitating a direct contact between the plasma and the liquid. This is an intriguing finding, as it is often assumed that direct-contact plasma systems offer a significantly more efficient means of degrading chemical pollutants due to the ability of short-lived chemical species to reach the liquid interface.

## 4. Conclusions

In this study, the decolourisation of indigo carmine dye was examined using an SBD coupled to a falling film reactor. The focus of the study was to investigate various key factors that affect the decolourisation efficacy and compare the efficiency achieved under the most favourable operating conditions against other plasma and non-plasma based AOPs. The parameters examined included the reactor configuration, the discharge power, and the use of pulse modulation. Gas phase species were quantified using UV absorption and FTIR, revealing that the power dissipated in the plasma had a dramatic influence on the composition of the reactive species, which was found to directly impact the efficacy of the approach and the composition of the exposed liquid.

Ultimately, it was shown that an unsealed reactor employing PWM excitation of the plasma offered the highest decolourisation efficiency, reaching a $G_{50}$ value of 20.18 g/kWh. By altering the reactor sealing configuration in the continuous mode, the $G_{50}$ value was affected, varying from 18.94 g/kWh to 16.67 g/kWh for the sealed and unsealed configurations, respectively. The efficiency of the indirect SBD falling film reactor was found to compare favourably against many other plasma and non-plasma based AOPs. The results of this study clearly indicate that the combination of a SBD plasma source and falling film reactor forms an efficient method for the decomposition of recalcitrant chemical compounds, while offering several benefits over direct-contact plasma-based AOPs.

## Funding

This work was supported by the European Union's EU Framework Programme for Research and Innovation Horizon 2020 under Grant Agreement No. 861369 (innoveox.eu).

## Declaration of competing interest

The authors declare that they have no known competing financial interests or personal relationships that could have appeared to influence the work reported in this paper.

## Data availability

Data will be made available on request.

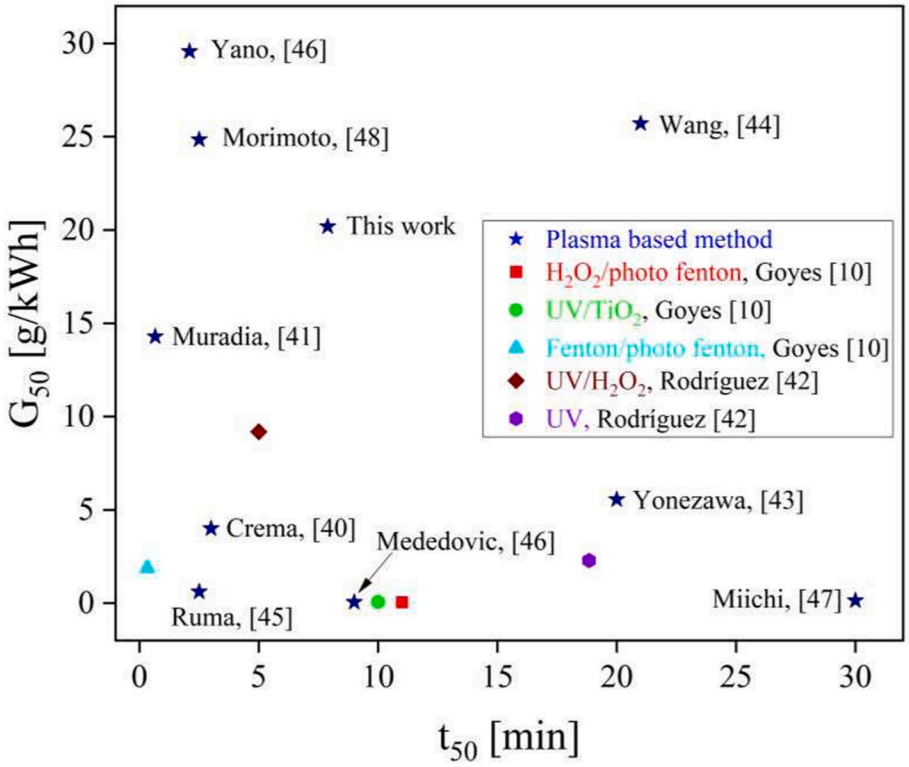


**Fig. 6.** Comparative study based on indigo carmine decolourisation efficiency ($G_{50}$) and the corresponding decolourisation time of various plasma-based (★) and non-plasma-based AOPs. (For interpretation of the references to colour in this figure legend, the reader is referred to the web version of this article.)

## Appendix A. Supplementary data

Supplementary data to this article can be found online at https://doi.org/10.1016/j.jwpe.2023.103632.

## References


[1] N. Barka, A. Assabbane, A. Nounah, Y.A. Ichou, Photocatalytic degradation of indigo carmine in aqueous solution by TiO2-coated non-woven fibres, J. Hazard. Mater. 152 (3) (2008) 1054–1059, https://doi.org/10.1016/j.jhazmat.2007.07.080.

[2] J.T. Spadaro, L. Isabelle, V. Renganathan, Hydroxyl radical mediated degradation of azo dyes: evidence for benzene generation, Environ. Sci. Technol. 28 (7) (1994) 1389–1393, https://doi.org/10.1021/es00056a031.

[3] W.C. Jeffords, D.L. Lance, P.H. Dewolf, Severe indigo, Urology IX (2) (1977) 180–181.

[4] E. Butrón, M.E. Juárez, M. Solis, M. Teutli, I. González, J.L. Nava, Electrochemical incineration of indigo textile dye in filter-press-type FM01-LC electrochemical cell using BDD electrodes, Electrochim. Acta 52 (24) (2007) 6888–6894, https://doi.org/10.1016/j.electacta.2007.04.108.

[5] M. Cai, M. Jin, L.K. Weavers, Analysis of sonolytic degradation products of azo dye Orange G using liquid chromatography-diode array detection-mass spectrometry, Ultrason. Sonochem. 18 (5) (2011) 1068–1076, https://doi.org/10.1016/j.ultsonch.2011.03.010.

[6] P. Bansal, D. Singh, D. Sud, Photocatalytic degradation of azo dye in aqueous TiO2 suspension: reaction pathway and identification of intermediates products by LC/MS, Sep. Purif. Technol. 72 (3) (2010) 357–365, https://doi.org/10.1016/j.seppur.2010.03.005.

[7] M.F. Chowdhury, S. Khandaker, F. Sarker, A. Islam, M.T. Rahman, M.R. Awual, Current treatment technologies and mechanisms for removal of indigo carmine dyes from wastewater: a review, J. Mol. Liq. 318 (2020), 114061, https://doi.org/10.1016/j.molliq.2020.114061.

[8] Y. Deng, R. Zhao, Advanced oxidation processes (AOPs) in wastewater treatment, Curr. Pollut. Rep. 1 (3) (2015) 167–176, https://doi.org/10.1007/s40726-015-0015-z.

[9] P.V. Nidheesh, M. Zhou, M.A. Oturan, An overview on the removal of synthetic dyes from water by electrochemical advanced oxidation processes, Chemosphere 197 (2018) 210–227, https://doi.org/10.1016/j.chemosphere.2017.12.195.

[10] R.E. Palma-Goyes, J. Silva-Agredo, I. González, R.A. Torres-Palma, Comparative degradation of indigo carmine by electrochemical oxidation and advanced oxidation processes, Electrochim. Acta 140 (2014) 427–433, https://doi.org/10.1016/j.electacta.2014.06.096.

[11] M.A. Malik, Water purification by plasmas: which reactors are most energy efficient? Plasma Chem. Plasma Process. 30 (1) (2010) 21–31, https://doi.org/10.1007/s11090-009-9202-2.

[12] M. Hijosa-Valsero, R. Molina, A. Montràs, M. Müller, J.M. Bayona, Decontamination of waterborne chemical pollutants by using atmospheric pressure nonthermal plasma: a review, Environ. Technol. Rev. 3 (1) (2014) 71–91, https://doi.org/10.1080/21622515.2014.990935.

[13] K. Kyere-Yeboah, I.K. Bique, X. Chen Qiao, Advances of non-thermal plasma discharge technology in degrading recalcitrant wastewater pollutants. A comprehensive review, Chemosphere 320 (January) (2023), 138061, https://doi.org/10.1016/j.chemosphere.2023.138061.

[14] C. Tendero, C. Tixier, P. Tristant, J. Desmaison, P. Leprince, Atmospheric pressure plasmas: a review, Spectrochim. Acta B At. Spectrosc. 61 (1) (2006) 2–30, https://doi.org/10.1016/j.sab.2005.10.003.

[15] J. Chen, J.H. Davidson, Ozone production in the positive DC Corona discharge: model and comparison to experiments, Plasma Chem. Plasma Process. 22 (4) (2002) 495–522, https://doi.org/10.1023/A:1021315412208.

[16] J. Chen, P. Wang, Effect of relative humidity on electron distribution and ozone production by DC coronas in air, IEEE Trans. Plasma Sci. 33 (2 II) (2005) 808–812, https://doi.org/10.1109/TPS.2005.844530.

[17] B.R. Locke, M. Sato, P. Sunka, M.R. Hoffmann, J.S. Chang, Electrohydraulic discharge and nonthermal plasma for water treatment, Ind. Eng. Chem. Res. 45 (3) (2006) 882–905, https://doi.org/10.1021/ie050981u.

[18] D.X. Liu, Z.C. Liu, C. Chen, A.J. Yang, D. Li, M.Z. Rong, H.L. Chen, M.G. Kong, Aqueous reactive species induced by a surface air discharge: heterogeneous mass transfer and liquid chemistry pathways, Sci. Rep. 6 (April) (2016) 1–11, https://doi.org/10.1038/srep23737.

[19] T. Wang, G. Qu, J. Ren, Q. Sun, D. Liang, S. Hu, Organic acids enhanced decoloration of azo dye in gas phase surface discharge plasma system, J. Hazard. Mater. 302 (2016) 65–71, https://doi.org/10.1016/j.jhazmat.2015.09.051.

[20] T. Wang, H. Jia, X. Guo, T. Xia, G. Qu, Q. Sun, X. Yin, Evaluation of the potential of dimethyl phthalate degradation in aqueous using sodium percarbonate activated by discharge plasma, Chem. Eng. J. 346 (2018) 65–76, https://doi.org/10.1016/j.cej.2018.04.024.

[21] P.K. Pandis, C. Kalogirou, E. Kanellou, C. Vaitsis, M.G. Savvidou, G. Sourkouni, A. A. Zorpas, C. Argirusis, Key points of Advanced Oxidation Processes (AOPs) for wastewater, organic pollutants and pharmaceutical waste treatment: a mini review, ChemEngineering 6 (1) (2022), https://doi.org/10.3390/chemengineering6010008.

[22] B. Jiang, J. Zheng, S. Qiu, M. Wu, Q. Zhang, Z. Yan, Q. Xue, Review on electrical discharge plasma technology for wastewater remediation, Chem. Eng. J. 236 (2014) 348–368, https://doi.org/10.1016/j.cej.2013.09.090.

[23] K. Shang, R. Morent, N. Wang, Y. Wang, B. Peng, N. Jiang, N. Lu, J. Li, Degradation of sulfamethoxazole (SMX) by water falling film DBD plasma/persulfate: reactive

species identification and their role in SMX degradation, Chem. Eng. J. 431 (September) (2021) 2022, https://doi.org/10.1016/j.cej.2021.133916.
[24] G.R. Stratton, C.L. Bellona, F. Dai, T.M. Holsen, S.M. Thagard, Plasma-based water treatment: conception and application of a new general principle for reactor design, Chem. Eng. J. 273 (2015) 543–550, https://doi.org/10.1016/j.cej.2015.03.059.
[25] N. Ghasemi, F. Zare, H. Hosano, A review of pulsed power Systems for Degrading Water Pollutants Ranging from microorganisms to organic compounds, IEEE Access 7 (2019) 150863–150891, https://doi.org/10.1109/ACCESS.2019.2947632.
[26] P. Bruggeman, C. Leys, Non-thermal plasmas in and in contact with liquids, J. Phys. D. Appl. Phys. 42 (5) (2009), https://doi.org/10.1088/0022-3727/42/5/053001.
[27] A. Kumar, N. Škoro, W. Gernjak, D. Povrenović, N. Puač, P. Attri, D. Boonyawan, U. Narayan, in: Direct and Indirect Treatment of Organic Dye (Acid Blue 25) Solutions by Using Cold Atmospheric Plasma Jet vol. 10, 2022, p. 1, https://doi.org/10.3389/fphy.2022.835635. Article.
[28] K.H. Hama Aziz, H. Miessner, S. Mueller, A. Mahyar, D. Kalass, D. Moeller, I. Khorshid, M.A.M. Rashid, Comparative study on 2,4-dichlorophenoxyacetic acid and 2,4-dichlorophenol removal from aqueous solutions via ozonation, photocatalysis and non-thermal plasma using a planar falling film reactor, J. Hazard. Mater. 343 (2018) 107–115, https://doi.org/10.1016/j.jhazmat.2017.09.025.
[29] Z. Kozakova, E.J. Klimova, B.M. Obradovic, B.P. Dojcinovic, F. Krcma, M. M. Kuraica, Z. Olejnickova, R. Sykora, M. Vavrova, Comparison of liquid and liquid-gas phase plasma reactors for discoloration of azo dyes: analysis of degradation products, Plasma Process. Polym. 15 (6) (2018), https://doi.org/10.1002/ppap.201700178.
[30] K. Takahashi, S. Kawamura, I. Yagi, M. Akiyama, K. Takaki, N. Satta, Influence of reactor geometry and electric parameters on wastewater treatment using discharge inside a bubble, Int. J. Plasma Environ. Sci. Technol. 13 (2) (2019) 74–82.
[31] P.T.T. Le, C.E. Boyd, Comparison of phenate and salicylate methods for determination of Total ammonia nitrogen in freshwater and saline water, J. World Aquac. Soc. 43 (6) (2012) 885–889, https://doi.org/10.1111/j.1749-7345.2012.00616.x.
[32] T. Yano, N. Shimomura, I. Uchiyama, F. Fukawa, K. Teranishi, H. Akiyama, Decolorization of indigo carmine solution using nanosecond pulsed power, IEEE Trans. Dielectr. Electr. Insul. 16 (4) (2009) 1081–1087, https://doi.org/10.1109/TDEI.2009.5211858.
[33] H. Kobayashi, T. Tandou, H. Nagaishi, W. Xi, W. Wang, Z. Liu, T. Shimizu, Y. Sakiyama, D.B. Graves, J.L. Zimmermann, G.E. Morfill, The dynamics of ozone generation and mode transition in air surface micro-discharge plasma at atmospheric pressure You may also like Decrease in Ozone Density of Atmospheric Surface-Discharge Plasma Source The dynamics of ozone generation and mode transition in air surface micro-discharge plasma at atmospheric pressure, al -, New J. Phys. 14 (11) (2012) 103028, https://doi.org/10.1088/1367-2630/14/10/103028.
[34] T. Shimizu, Y. Sakiyama, D.B. Graves, J.L. Zimmermann, G.E. Morfill, The dynamics of ozone generation and mode transition in air surface micro-discharge plasma at atmospheric pressure, New J. Phys. 14 (2012), https://doi.org/10.1088/1367-2630/14/10/103028.
[35] S. Park, W. Choe, C. Jo, Interplay among ozone and nitrogen oxides in air plasmas: rapid change in plasma chemistry, Chem. Eng. J. 352 (February) (2018) 1014–1021, https://doi.org/10.1016/j.cej.2018.07.039.
[36] M.J. Pavlovich, D.S. Clark, D.B. Graves, Quantification of air plasma chemistry for surface disinfection, Plasma Sources Sci. Technol. 23 (6) (2014), https://doi.org/10.1088/0963-0252/23/6/065036.
[37] S. Park, W. Choe, C. Jo, Interplay among ozone and nitrogen oxides in air plasmas: rapid change in plasma chemistry, Chem. Eng. J. 352 (February) (2018) 1014–1021, https://doi.org/10.1016/j.cej.2018.07.039.
[38] S.P. Tan, M. Piri, Modeling the solubility of nitrogen dioxide in water using perturbed-chain statistical associating fluid theory, Ind. Eng. Chem. Res. 52 (45) (2013) 16032–16043, https://doi.org/10.1021/ie402417p.
[39] T. Handa, Y. Minamitani, The effect of a water-droplet spray and gas discharge in water treatment by pulsed power, IEEE Trans. Plasma Sci. 37 (1) (2009) 179–183, https://doi.org/10.1109/TPS.2008.2007729.
[40] S. Muradia, M. Nagatsu, Low-voltage pulsed plasma discharges inside water using a bubble self-generating parallel plate electrode with a porous ceramic, Appl. Phys. Lett. 102 (14) (2013), https://doi.org/10.1063/1.4799652.
[41] A.P.S. Crema, L.D. Piazza Borges, G.A. Micke, N.A. Debacher, Degradation of indigo carmine in water induced by non-thermal plasma, ozone and hydrogen peroxide: a comparative study and by-product identification, Chemosphere 244 (2020), 125502, https://doi.org/10.1016/j.chemosphere.2019.125502.
[42] E. Rodríguez, R. Peche, J.M. Merino, L.M. Camarero, Decoloring of aqueous solutions of indigocarmine dye in an acid medium by H2O2/UV advanced oxidation, Environ. Eng. Sci. 24 (3) (2007) 363–371, https://doi.org/10.1089/ees.2006.0023.
[43] M. Yonezawa, K. Murata, K. Teranishi, N. Shimomura, Decolorization of indigo carmine solution by argon dielectric barrier discharge produced on liquid surface, Jpn. J. Appl. Phys. 58 (12) (2019), https://doi.org/10.7567/1347-4065/ab5605.
[44] Z.H. Wang, D.X. Xu, G. Zhang, The energy efficiency analysis of dye decoloration by spraying discharge plasma, Adv. Mater. Res. 830 (2014) 388–391, https://doi.org/10.4028/www.scientific.net/AMR.830.388.
[45] Ruma, H. Hosano, T. Sakugawa, H. Akiyama, The role of pulse voltage amplitude on chemical processes induced by streamer discharge at water surface, Catalysts 8 (5) (2018) 2–13, https://doi.org/10.3390/catal8050213.
[46] S. Mededovic, K. Takashima, Decolorization of indigo carmine dye by spark discharge in water, Int. J. Plasma Environ. Sci. Technol. 2 (1) (2008) 56–64.
[47] T. Miichi, Decolonization of indigo carmine solution using discharge on surface of a gas-layer in water, IEEJ Trans. Fundam. Mater. 126 (8) (2006) 851–856, https://doi.org/10.1541/ieejfms.126.851.
[48] M. Morimoto, K. Shimizu, K. Teranishi, N. Shimomura, Indigo carmine solution treatment by nanosecond pulsed power with a dielectric barrier electrode, IEEE Trans. Dielectr. Electr. Insul. 22 (4) (2015) 1872–1878, https://doi.org/10.1109/TDEI.2015.004960.